PHYSICAL REVIEW A VOLUME 46, NUMBER 8 15 OCTOBER 1992

Neutron-diffraction study of liquid hydrogen iodide

C. Andreani
Dipartimento di Fisica, Università di Tor Vergata, Roma, Italy

M. Nardone and F. P. Ricci
Dipartimento di Fisica, Università "La Sapienza," Roma, Italy

A. K. Soper
Rutherford Appleton Laboratory, Chilton Didcot OX11 0QX, England

(Received 16 April 1992)

Neutron-diffraction experiments on liquid DI, HI, and on an equimolar mixture of HI and DI are presented. All these three samples were in the same thermodynamic state corresponding to the orthobaric liquid at $T=253$ K. The three partial structure factors $S_{\rm II}(Q)$, $S_{\rm HI}(Q)$, $S_{\rm HH}(Q)$ are derived exploiting the standard isotopic substitution procedure. The corresponding pair correlation functions $g_{\rm II}(r)$, $g_{\rm HI}(r)$, and $g_{\rm HH}(r)$ are evaluated and compared with those given by a model that neglects all orientational correlations. Our data indicate that $g_{\rm II}(r)$ (which is essentially the center-center correlation function) is well reproduced by the pair distribution function of a monatomic Lennard-Jones fluid and that $g_{\rm HI}(r)$ (which should be sensitive to the correlations between molecular and intermolecular axes) is very similar to the one derived neglecting orientational correlations. On the contrary, orientational correlations between the molecular axes are clearly present in the $g_{\rm HH}(r)$, which deviates significantly from the uncorrelated model results. These facts are consistent with the idea that H bonding is not present in liquid HI and indicate also that the only relevant terms of the anisotropic intermolecular potential are those due to the electric multipolar interactions.

PACS number(s): 61.20.−p, 61.12.Ex, 61.12.Gz

INTRODUCTION

Among diatomic liquids the hydrogen halides are particularly interesting because while the repulsive hard-core interactions due to electronic overlap can be assumed to be almost isotropic throughout the series, the anisotropic interactions (such as those due to multipolar contributions, charge transfer, and polarization forces) become increasingly important in going to the lighter halides. As a matter of fact, hydrogen bonding is generally assumed [1] to be clearly present in HF, to a small degree in HCl and should be practically absent in HBr and HI. However structural information obtained by neutron-diffraction measurements is somewhat conflicting. A set of experimental determinations of the total structure factor in liquid DF [2], DCl [4], and DBr [5] gave radial distribution functions $g(r)$ that exhibit a peak interpreted by the authors as due to H bonds. This peak is present beyond any doubt in HF while it became less clearly determined in going to the heavier halides. Moreover another neutron-diffraction measurement on liquid HCl has been performed [3] in which the three partial structure factors were determined by isotope substitution, but these did not bring further evidence to support the existence of H bonds. It seems therefore worthwhile to determine experimentally the partial structure factors for all the halogen halides at the same corresponding thermodynamic state. In particular the understanding of the structure of liquid HI near the melting point is the necessary first step since the expected weakness of H bonds should allow us to investigate the structural effects of the anisotropic terms of the intermolecular potential, namely the multipolar electrostatic terms, which are present in all halogen halides.

However to our knowledge, there are no x-ray or neutron-diffraction data on this system. For this reason, neutron-diffraction measurements have been performed on liquid HI and DI and on an equimolar mixture of HI and DI (hereafter labeled HDI). All these three samples were in the same thermodynamic state corresponding to the orthobaric liquid at $T=253$ K (molecular number density $\rho=0.0123$ molecules/Å^3). The partial structure factors obtained following the data reduction described in the next section will be used to investigate the presence of hydrogen bonding and to clarify the kind of orientational correlations present in the liquid. The discussion of the atom-atom partial structure factors in terms of orientational correlation turns out to be particularly simple in the case of the hydrogen halides since the coordinates of the halogen atom are practically coincident with those of the molecular center of mass.

THEORETICAL BACKGROUND

General formalism

We will assume that the measured differential scattering cross section per molecule can be written as

$$\left[\frac{\partial\sigma}{\partial\Omega}\right]=F(Q)+\frac{1}{4\pi}\sum_{\alpha}\sigma_{s,\alpha}[1+P_\alpha(Q)]\ , \qquad (1a)$$

where $P_\alpha(Q)$ is the inelasticity correction to the self-scattering contribution of atomic species α and

$$F(Q)=\sum_{\alpha,\beta} b_\alpha b_\beta [S_{\alpha\beta}(Q)-\delta_{\alpha\beta}] \ , \tag{1b}$$

where b_α and $\sigma_{s\alpha}$ are, respectively, the coherent scattering length and total scattering cross section of species α (see Table I). The partial structure factors $S_{\alpha\beta}(Q)$ are defined in terms of the pair distribution functions $g_{\alpha\beta}(r)$ to be

$$S_{\alpha\beta}(Q)-\delta_{\alpha\beta}=\rho \int [g_{\alpha\beta}(r)-1]e^{i\mathbf{Q}\cdot\mathbf{r}}d\mathbf{r} \ . \tag{2}$$

Assuming Eq. (1a) we have neglected inelasticity corrections to the interference scattering function $F(Q)$.

The partial structure factors contain, generally speaking, both intermolecular and intramolecular contributions so that we may write

$$S_{\alpha\beta}(Q)=S_{\alpha\beta}^{\text{inter}}(Q)+S_{\alpha\beta}^{\text{intra}}(Q) \ . \tag{3}$$

In the case of heteronuclear diatomics

$$S_{\alpha\beta}^{\text{intra}}(Q)=\begin{cases} 1 \quad \text{if } \alpha=\beta \\ \langle e^{i\mathbf{Q}\cdot(\mathbf{r}_{1\alpha}-\mathbf{r}_{1\beta})}\rangle \cong \dfrac{\sin QR}{QR}e^{-1/2\langle u^2\rangle Q^2} \quad \text{if } \alpha\neq\beta \ , \end{cases} \tag{4a}$$

$$S_{\alpha\beta}^{\text{inter}}(Q)=N\langle e^{i\mathbf{Q}\cdot(\mathbf{r}_{1\alpha}-\mathbf{r}_{2\beta})}\rangle \ , \tag{4b}$$

where the angular brackets indicate thermal averages, $\mathbf{r}_{i\alpha}$ the position of atom α belonging to molecule i, R the intramolecular distance, $\langle u^2\rangle$ its mean-square displacement, and N the total number of molecules.

It can be shown from Eq. (2) that

$$S_{\alpha\beta}(0)=\rho k_B T \chi_T \tag{5}$$

χ_T being the isothermal compressibility and k_B the Boltzmann constant.

In terms of our previous definitions, the total intermolecular structure factor $D(Q)$, often used to describe average intermolecular interference effects, is given by

$$\begin{aligned} D(Q) &= \left[\sum_\alpha b_\alpha\right]^{-2} F^{\text{inter}}(Q) \\ &= \left[\sum_\alpha b_\alpha\right]^{-2} \sum_{\alpha,\beta} b_\alpha b_\beta S_{\alpha\beta}^{\text{inter}}(Q) \ , \end{aligned} \tag{6a}$$

where

$$D(0)=\left[\sum_\alpha b_\alpha\right]^{-2} F^{\text{inter}}(0)=\rho k_B T X_T - 1 \ . \tag{6b}$$

TABLE I. Atomic parameters for I, H, and D.

Species	$b_\alpha \times 10^{12}$ cm	$\sigma_{s\alpha}$ (10^{-24} cm^2)	M_α (a.u.)
I	0.528	4.52	126.9
H	−0.374	81.67	1.008
D	0.667	7.63	2.00

TABLE II. Partial structure factor weighting coefficients as defined by Eq. (7).

$\alpha\beta$	$A_{\alpha\beta}$	$B_{\alpha\beta}$	$C_{\alpha\beta}$
II	0.649	−0.364	3.311
HH=DD	1.852	1.852	−3.704
HI=DI	−1.414	0.397	1.025

In the alkali halides, under the reasonable assumption that the local structure is not affected by deuteration, one can extract the intermolecular partial structure factors from the $F^{\text{inter}}(Q)$ functions obtained from three samples with different deuterium content. In particular the three partials can be written as linear combinations of the three measured $F^{\text{inter}}(Q)$:

$$\begin{aligned} S_{\alpha\beta}^{\text{inter}}(Q) = {} & A_{\alpha\beta}F_{\text{HI}}^{\text{inter}}(Q)+B_{\alpha\beta}F_{\text{DI}}^{\text{inter}}(Q) \\ & +C_{\alpha\beta}F_{\text{HI}}^{\text{inter}}(Q) \ . \end{aligned} \tag{7}$$

The weighting coefficients appropriate for our experiment are reported in Table II.

Orientational correlations

In a diatomic molecular fluid the atomic positions $\mathbf{r}_{i\alpha}$ can be written in terms of the center-of-mass coordinates $\mathbf{r}_{ic}$ of the ith molecule and of the unit vectors $\mathbf{u}_i$ describing the orientation of its axis to yield

$$\mathbf{r}_{i\alpha}=\mathbf{r}_{ic}+R_\alpha \mathbf{u}_i \ , \tag{8}$$

R_α being the distance between atom α and the molecular center of mass.

In view of the large mass ratio between iodine and hydrogen (or deuterium) atoms, we will assume

$$R_{\text{I}}\approx 0, \quad R_{\text{H}}=R_{\text{D}}\approx R \ , \tag{9}$$

so that we can write

$$S_{\text{II}}^{\text{inter}}(Q)\approx N\langle e^{i\mathbf{Q}\cdot(\mathbf{r}_{1c}-\mathbf{r}_{2c})}\rangle = S_{cc}(Q)-1 \ , \tag{10a}$$

$$S_{\text{HH}}^{\text{inter}}(Q)\approx N\langle e^{i\mathbf{Q}\cdot(\mathbf{r}_{1c}-\mathbf{r}_{2c})}e^{iR\mathbf{Q}\cdot(\mathbf{u}_1-\mathbf{u}_2)}\rangle \ , \tag{10b}$$

$$S_{\text{IH}}^{\text{inter}}(Q)\approx N\langle e^{i\mathbf{Q}\cdot(\mathbf{r}_{1c}-\mathbf{r}_{2c})}e^{iR\mathbf{Q}\cdot\mathbf{u}_1}\rangle \ , \tag{10c}$$

where $S_{cc}(Q)$ is the structure factor for the molecular centers of mass. The averages appearing in Eqs. (10b) and (10c) can be calculated using the pair correlation function $g(\mathbf{r}_{12},\omega_1,\omega_2)$ [6], being

$$\langle B\rangle = \frac{1}{V}\frac{1}{(4\pi)^2}\int Bg(\mathbf{r}_{12},\omega_1,\omega_2)d\mathbf{r}_{12},d\omega_1,d\omega_2 \ ,$$

where $\omega_i \equiv (\theta_i\phi_i)$ describes the orientation of molecule i with respect to the space fixed axes.

If orientational correlations are neglected altogether and the system is isotropic,

$$g(\mathbf{r}_{12},\omega_1,\omega_2)=g_{cc}(r_{12}) \ ,$$

where $g_{cc}(r_{12})$ is the center-of-mass pair distribution function. The uncorrelated model yields therefore

$$S_{\mathrm{HH}}^{\mathrm{inter}}(Q)=[S_{cc}(Q)-1]\left[\frac{\sin QR}{QR}\right]^2 , \qquad (11a)$$

$$S_{\mathrm{HH}}^{\mathrm{inter}}(Q)=[S_{cc}(Q)-1]\left[\frac{\sin QR}{QR}\right] , \qquad (11b)$$

where we have neglected the Debye-Waller factors arising from vibrational motions owing to the limited-Q range in which $[S_{cc}(Q)-1)]$ is different from zero.

It should be noted that owing to the proximity of the molecular center of mass to the iodine atom, $S_{\mathrm{HI}}(Q)$ is sensitive only to correlations between the orientations of the molecular axis and the intermolecular vector r_{12}. It will therefore reduce to the uncorrelated model result [Eq. (11b)] when these correlations are weak. Not much can be said *a priori* on the existence of this kind of correlation in fluid HI except that if H bonding is present these correlations should be relevant.

On the contrary $S_{\mathrm{HH}}(Q)$ is sensitive also to correlations between the molecular axes of different molecules. These are certainly present in fluid HI since the value of the static dielectric constant allows us to evaluate the Kirkwood correlation factor to be [7]

$$g=1+N\langle \mathbf{u}_1\cdot\mathbf{u}_2\rangle \cong 2 .$$

Therefore the uncorrelated model is bound to be only a crude approximation for $S_{\mathrm{HH}}(Q)$.

EXPERIMENTAL PROCEDURE AND DATA ANALYSIS

The experiment has been performed on the spallation neutron source ISIS at the Rutherford Appleton Laboratory (UK) using the small-angle neutron diffractometer for liquid and amorphous samples (SANDALS) spectrometer [8]. The DI sample was contained in a thin-walled (0.1 cm) rectangular cell made of TiZr with 4.4×2 cm^2 area exposed to the neutron beam and 0.7 cm internal width. Due to the large scattering cross section of hydrogen, HI and HDI samples were both contained in another TiZr cell, having internal width of 0.2 cm.

Pure HI and DI were condensed from the lecture bottles directly into the cell. The HDI sample was previously prepared in a reservoir bottle, homogenized and then condensed into the cell. The temperature of the samples was held fixed at 253±0.5 K by a closed-cycle refrigerator; the temperature difference between the top and the bottom of the cell, controlled by two thermocouples, turned out to be less than 1 K.

The pressure was read by a strain gauge with an accuracy of ±2 kPa and kept slightly higher than the vapor pressure to avoid bubbling due to local thermal instabilities. During each measurement it remained constant within 10 kPa.

Neutrons diffracted from liquid samples (HI, DI, HDI) empty containers, vanadium, and background were collected as a function of the neutron time of flight at eight scattering angles: (±20.13°, 18.11°, 16.23°, 14.61°). For each spectrum various runs were recorded in blocks lasting typically three hours in order to check the reproducibility of the measurements; they turned out to coincide within their statistical accuracy.

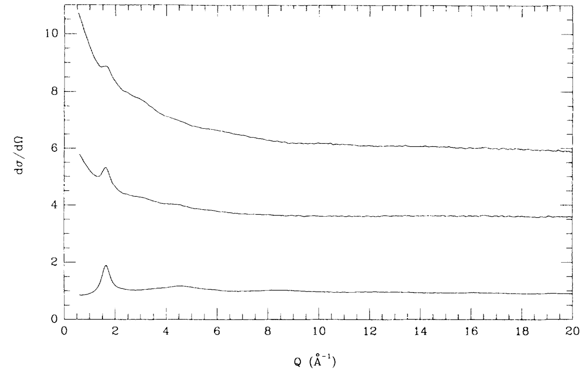

FIG. 1. Differential scattering cross section per molecule (averaged over all detectors) as a function of the exchanged wave vector Q for the three measured samples.

The time-of-flight spectra of the three samples, empty can, and vanadium have been corrected for background intensity multiple scattering, absorption, and when necessary for empty can contributions. Moreover the time of flight has been converted into the elastic exchanged wave vector Q. All these operations have been done following the procedure described in the ATLAS manual [9]. For each Q value the intensity has been put on absolute basis using the vanadium spectra.

The differential scattering cross sections per molecule, averaged over all detectors, are reported in Fig. 1. Figure 1 shows that at a high-exchanged wave vector, the differential cross sections are of the order of $\sigma_s/4\pi$ for all three samples. This is to be expected since, due to the rather low scattering angles adopted by SANDALS, only high-energy incident neutrons can contribute in this momentum range and consequently inelasticity corrections are relatively small. On the contrary in the low-Q region the effects due to inelasticity become increasingly important particularly in the hydrogen-rich samples. The figure shows also that while the intermolecular interference peak at about 1.7 Å^{-1} is clearly visible in all three samples, the intramolecular interference, high-Q oscillations are visible only in the DI spectrum.

This is due to the relatively large value of $2b_{\mathrm{I}}b_{\mathrm{D}}$ (0.705×10^{-24} cm^2) compared to the corresponding values for the other samples (namely, -0.395×10^{-24} cm^2 for HI and 0.155×10^{-24} cm^2 for HDI) and to the relatively small inelasticity corrections in DI, where the atomic self-scattering appears as an almost flat background in the range of interest.

In order to obtain from the data in Fig. 1 the $F(Q)$ required to derive structural information on the fluid, one must now get rid of the inelasticity-corrected atomic self-scattering corresponding to the second term on the right-hand side of Eq. (1a). Unfortunately a rigorous analytical treatment of the inelasticity corrections is not available for light atoms such as hydrogen and deuterium, we will therefore cope with this problem exploiting the "ansatz" that the self-scattering is a smooth decreasing function of Q, as suggested by Fig. 1.

The procedure we have adopted, after checking that

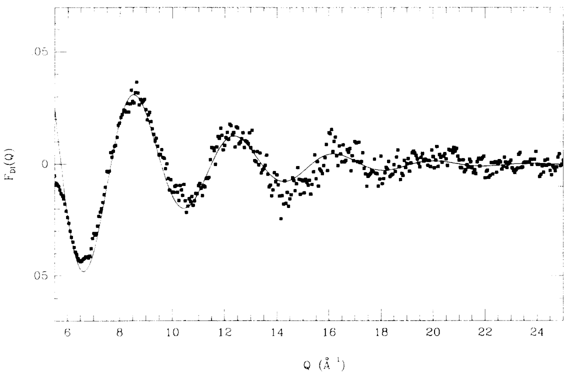

FIG. 2. Interference scattering function for the DI sample, as a function of Q in the range in which the intramolecular interference is largely predominant. Experimental points, ■; best fit using Eq. (4a) (——).

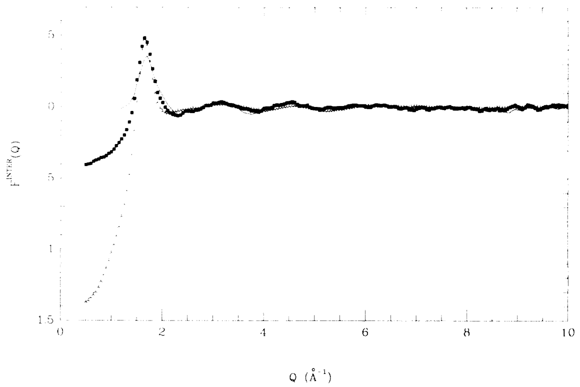

FIG. 3. Intermolecular scattering functions, as a function of Q for the three measured samples. HI(——), DI(⅄), HDI(■).

consistent results are obtained for each of the quoted detectors, is the following.

(i) We first derive the molecular parameters R and $\langle u^2 \rangle$ from the high-Q region of the DI spectrum.

(ii) We then subtract the appropriate intramolecular contributions from the three differential cross sections of Fig. 1.

(iii) We finally fit these resulting cross sections, excluding the region where strong intermolecular structural interference is present, with a simple analytical function accounting for both high- and low-Q limits of $F(Q)$. This function that is assumed to represent the atomic self-scattering is then subtracted from the cross sections in order to obtain $F^{\text{inter}}(Q)$.

In particular the effective molecular parameters are obtained [point (i)] fitting by means of a MINUIT [10] routine the 7–25 Å^{-1} range of the DI spectrum accounting for the smooth background by a low-order polynomial (see Fig. 2). The value obtained for R lies in the 1.61–1.64 Å range, while $\langle u^2 \rangle$ is of the order of 0.013 Å^2.

As far as the value of R is concerned, our result is consistent with the gas-phase value of 1.609 Å [11], although it suggests the presence of more elongated bonds in the liquid phase even if one allows for anharmonicity of zero-point vibrations. Similar results have also been found in DBr [5]. The value of $\langle u^2 \rangle$ is rather larger than the one calculated from the knowledge of the vibrational frequency ω_v ($\langle u^2 \rangle = h/2m\omega_v \simeq 5\times 10^{-3}$ Å^2), but we must recall that it represents an effective Debye-Waller amplitude [5].

In subtracting the intramolecular interference term from the HI and the HDI spectra [point (ii)] we have accounted for the different molecular vibrational frequencies by appropriately scaling the value of $\langle u^2 \rangle$, although this appears to be immaterial as far as the resulting $F^{\text{inter}}(Q)$s are concerned.

As far as the inelasticity-corrected atomic self-scattering is concerned [point (iii)], we have found that in the range which is of interest to intermolecular interference effects (namely 0–15 Å), self-scattering could be satisfactorily accounted for assuming

$$\frac{1}{4\pi}\sum_{\alpha}\sigma_{s\alpha}[1+P_\alpha(Q)] = a + be^{-\lambda_1 Q} + ce^{-\lambda_2 Q^2} \ . \quad (12)$$

For each spectrum, the parameter a should be approximately given by the appropriate value of $\sigma_s/4\pi$, in agreement with the requirement

$$\lim_{Q\to\infty} F^{\text{inter}}_{(Q)} = 0 \ , \quad (13)$$

while the sum $(a+b+c)$ should be determined fulfilling Eq. (6b). In particular with $\rho k_B T \chi_T \ll 1$ [12], we must have

$$F^{\text{inter}}_{(0)} = -\left[\sum_\alpha b_\alpha\right]^2 . \quad (14)$$

The totally free parameters λ_1 and λ_2 describe, respectively, the slow high-Q and the steeper low-Q decay observed in Fig. 1.

The parameters are obtained fitting by means of a MINUIT routine, Eq. (12) to the data in Fig. 1 in the 3–10 Å^{-1} range [according to Eq. (13)] and to the data plus $(\sum_\alpha b_\alpha)^2$ in the 0.6–1.2 Å^{-1} range [according to Eq. (14)].

The obtained $F^{\text{inter}}(Q)$ are reported in Fig. 3. The parameters describing the atomic self-scattering are given in Table III.

The partial intermolecular structure factors $S^{\text{inter}}_{\text{II}}(Q)$, $S^{\text{inter}}_{\text{HH}}(Q)$, $S^{\text{inter}}_{\text{HI}}(Q)$, calculated using Eq. (7) are reported, respectively, in Figs. 4(a), 4(b), and 4(c) and in Table IV.

In Fig. 4(a) we also report the structure factor of a Lennard-Jones (LJ) fluid obtained by molecular-dynamics simulation at $\rho^* = \rho\sigma^3 = 0.805$ and $T^* = k_B T/\varepsilon = 0.76$.

TABLE III. Parameters describing the atomic self-scattering as given by Eq. (11).

	a 10^{-24} cm^2	b 10^{-24} cm^2	c 10^{-24} cm^2	λ_1 (Å)	λ_2 (Å)^2
HI	5.96	4.23	2.17	0.31	1.10
HDI	3.55	2.20	0.88	0.37	0.96
DI	0.93	0.47	0.40	0.27	0.90

These values have been chosen so that when $\sigma = 4.05$ Å and $\varepsilon / k_B = 333$ K (as determined from the critical constants of HI, namely, $T_c \simeq 1.26 \varepsilon / k_B$ and $P_c \simeq 12.2 \times 10^{-8} \varepsilon / \sigma^3$ atm), temperature and particle number density are those of our sample.

In Figs. 4(b) and 4(c) we also report for comparison the partial structure factors corresponding to the uncorrelated model of Eqs. (11a) and (11b) with $S_{cc}(Q)$ given by $S_{II}(Q)$ following Eq. (10a). Virtually identical results are obtained using for $S_{cc}(Q)$ the LJ fluid structure factor of Fig. 4(a).

The center-of-mass pair distribution function obtained inverting Eq. (2) and using Eq. (10a) is reported in Table V and in Fig. 5(a) together with the corresponding quantity for the LJ fluid. The HH and HI intermolecular pair distribution functions are reported in Table V and in Figs. 5(b) and 5(c) together with the corresponding quantities given by the uncorrelated model [see Eqs. (11a) and (11b)].

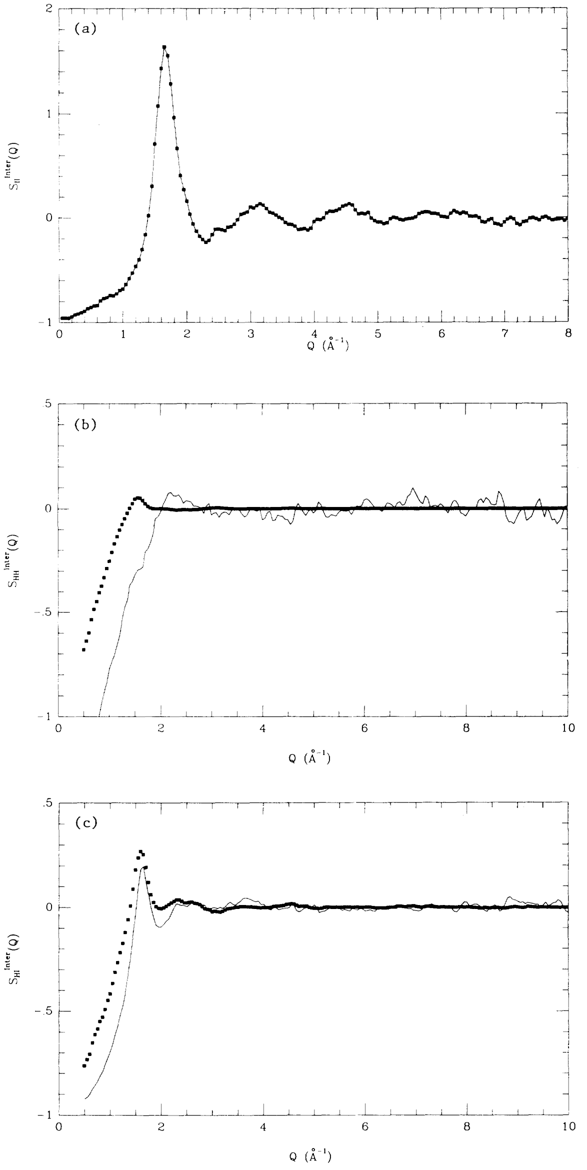

FIG. 4. (a) Iodine-iodine experimental partial structure factor (——) as determined using Eq. (7) and Table II. Structure factor of a LJ fluid (■), as determined by MD, using $\sigma = 4.05$ Å, $\varepsilon / k = 333$ K, and reduced state parameters $\rho^* = 0.805$ and $T^* = 0.76$. (b) Hydrogen-hydrogen experimental partial structure factor (——) and the prediction of the uncorrelated model [see Eq. (11b)] when $S_{II}(Q)$ is used to represent the center-of-mass structure factor (■). (c) Same as (b) for the hydrogen-iodine partial structure factor.

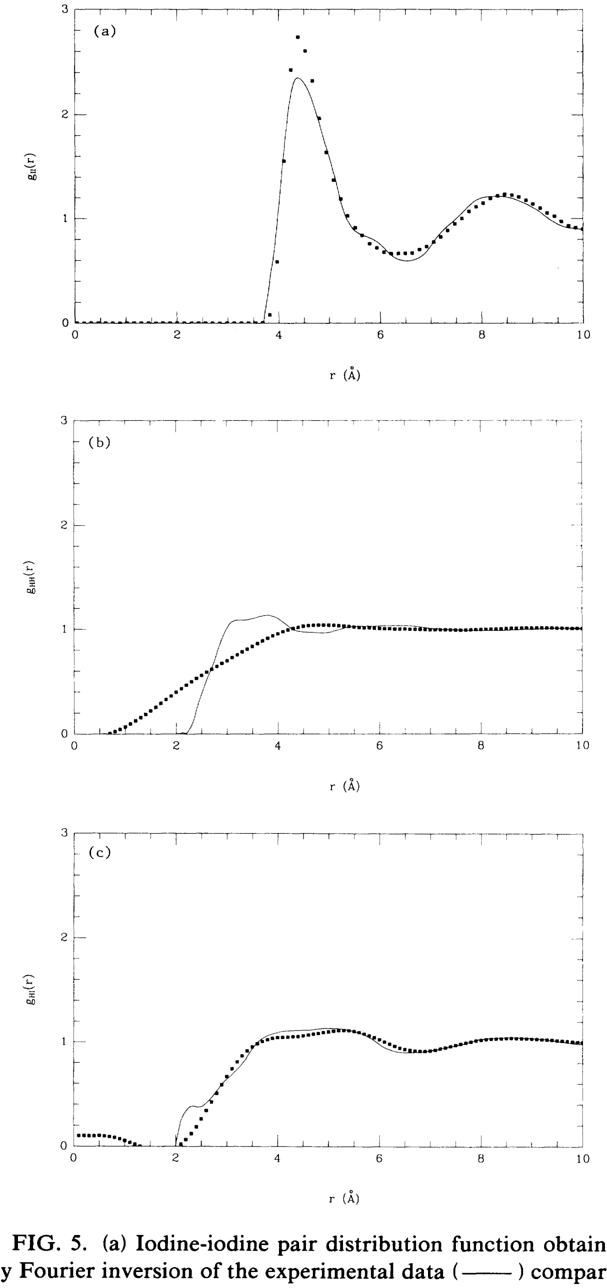

FIG. 5. (a) Iodine-iodine pair distribution function obtained by Fourier inversion of the experimental data (——) compared with the molecular-dynamics results for the LJ fluid of Fig. 4(a) (■). (b) Hydrogen-hydrogen experimental pair distribution function (——) compared with the uncorrelated model results (■) from Eq. (11a). (c) As above for the intermolecular hydrogen-iodine pair distribution function.

DISCUSSION

The first point we want to discuss is the absence of H bonding in liquid HI. In analyzing the neutron-total-diffraction data of DF [2], DCl [4], and DBr [5], the authors argued out that in these systems H bonding is revealed by the presence of a rather well-defined peak in the total radial distribution function. The ratio of the r value of this peak to the R value of the intramolecular bond length is an almost linear increasing function of R; if we extrapolate this behavior to the case of HI we expect to find the H-bond peak, if any, in $g_{\mathrm{HI}}(r)$ somewhere around $r \simeq 3.9$ Å. Figure 5(c) shows no evidence of such a peak. Therefore on the basis of the criterion suggested by the quoted total-diffraction measurements one ought to conclude that H bonding is practically absent in HI. This result is in agreement with the analysis of Ref. [1].

The second point we want to discuss concerns the orientational correlations in liquid HI and in particular the existence of correlations between the molecular orientational axes and the intermolecular axes and of those between orientational axes of different molecules. The similarity between both the $S_{\mathrm{HI}}(Q)$ (particularly as far as the first peak position is concerned) and $g_{\mathrm{HI}}(r)$ with the corresponding functions of the uncorrelated model [Figs. 4(c) and 5(c)] suggests that although anisotropic terms are certainly present in the intermolecular potential, correlations between the molecular axis and the intermolecular vector are rather weak. This is consistent with very weak or absent H bonds. As a matter of fact the distribution of H atoms around a given molecule is characterized by a broad first-neighbor peak and indicates a distance of closest approach (between the molecular center of mass and the H atoms) of about 2 Å. This value is consistent with the difference between the center-of-mass closest approach distance [deduced from Fig. 5(a) to be about 3.6 Å] and the intramolecular bond length.

The effect of the anisotropic part of the intermolecular potential appears to be also irrelevant in determining the correlations between centers of mass of HI molecules. Indeed Figs. 4(a) and 5(a) show that these are quite well reproduced by those of a monatomic LJ system with values of σ and ε chosen on the basis of critical point parameters. Similar results have been obtained by molecular dynamics simulation on HCl [13,3].

The effects of the anisotropic part of the intermolecular potential are on the contrary rather evident in the H-H correlation functions. Indeed Figs. 4(b) and 5(b) show

TABLE IV. Intermolecular partial structure factors of liquid HI.

Q	$S_{\mathrm{HH}}(Q)$	$S_{\mathrm{HI}}(Q)$	$S_{\mathrm{II}}(Q)$	Q	$S_{\mathrm{HH}}(Q)$	$S_{\mathrm{HI}}(Q)$	$S_{\mathrm{II}}(Q)$
0.50	−1.079	−0.923	−0.856	3.80	−0.006	0.031	−0.110
0.60	−1.058	−0.902	−0.837	3.90	−0.013	0.031	−0.118
0.70	−1.076	−0.860	−0.770	4.00	−0.053	0.016	−0.038
0.80	−0.999	−0.814	−0.744	4.10	−0.017	−0.010	−0.019
0.90	−0.881	−0.761	−0.729	4.20	−0.057	−0.001	0.046
1.00	−0.771	−0.697	−0.683	4.30	−0.030	−0.012	0.060
1.10	−0.709	−0.608	−0.581	4.40	−0.038	−0.006	0.084
1.20	−0.613	−0.519	−0.466	4.50	−0.053	−0.004	0.122
1.30	−0.476	−0.410	−0.306	4.60	−0.061	0.007	0.121
1.40	−0.368	−0.250	0.020	4.70	0.026	−0.022	0.035
1.50	−0.318	−0.032	0.710	4.80	−0.015	−0.005	0.036
1.60	−0.291	0.183	1.430	4.90	−0.013	0.000	−0.004
1.70	−0.208	0.129	1.552	5.00	−0.020	0.012	−0.043
1.80	−0.164	−0.002	0.962	5.20	−0.016	−0.020	−0.012
1.90	−0.048	−0.086	0.405	5.40	−0.032	0.003	−0.024
2.00	−0.018	−0.095	0.160	5.60	−0.011	−0.011	0.008
2.10	0.043	−0.067	−0.059	5.80	−0.007	−0.012	0.053
2.20	0.078	−0.029	−0.178	6.00	0.041	−0.019	0.011
2.30	0.061	0.018	−0.235	6.20	0.009	−0.019	0.064
2.40	0.052	0.009	−0.164	6.40	0.003	−0.008	0.043
2.50	0.038	0.003	−0.111	6.60	0.003	0.010	−0.001
2.60	0.032	0.022	−0.125	6.80	0.021	−0.004	−0.014
2.70	0.013	0.021	−0.086	7.00	0.078	−0.016	−0.046
2.80	0.001	0.013	−0.019	7.20	0.060	−0.005	−0.059
2.90	0.014	−0.010	0.042	7.40	0.014	−0.001	−0.009
3.00	−0.029	−0.001	0.104	7.60	−0.004	0.000	−0.001
3.10	−0.020	−0.007	0.116	7.80	0.036	−0.023	−0.022
3.20	−0.023	−0.006	0.121	8.00	−0.038	0.023	−0.011
3.30	−0.018	0.016	0.053	8.40	0.052	−0.022	−0.049
3.40	−0.008	0.015	0.027	8.80	−0.038	0.043	−0.052
3.50	−0.005	0.021	−0.010	9.20	−0.060	0.022	0.056
3.60	−0.024	0.043	−0.063	9.60	0.001	0.007	0.002
3.70	−0.032	0.043	−0.080	10.00	0.010	−0.025	0.046

that both $S_{\mathrm{HH}}(Q)$ and $g_{\mathrm{HH}}(r)$ are quite different from the corresponding quantities obtained from the uncorrelated model. As a matter of fact $S_{\mathrm{HH}}(Q)$ is sensitive both to correlations between the molecular symmetry axis and the intermolecular vector as well as to correlations between the molecular axes of different molecules. Since we have seen that the former are not particularly strong in fluid HI we must conclude that the main effect of the anisotropic intermolecular interactions is to produce a noticeable amount of the latter which also determines the value of the dielectric constant. As a matter of fact the distribution of H atoms around a given H atom displays a maximum at 3.5 Å, which is not present in the uncorrelated case that, on the contrary, displays only a broad feature centered around 4.5 Å, corresponding roughly to the center-of-mass first-neighbor distance. Moreover, Fig. 5(b) shows that the hydrogen-hydrogen closest-approach distance in liquid HI ($\sim$2 Å) is much larger than the one given by the uncorrelated model. Therefore, as a consequence of the orientational correlations in liquid HI, hydrogen atoms are on the average closer to each other than the iodine atoms but are restricted to stay at least 2 Å apart.

A similar effect although less pronounced was found also in HCl [3]. However since HCl was measured at $T/T_c \sim 0.9$ the results cannot be simply scaled to our HI data for which $T/T_c \sim 0.6$.

CONCLUSION

Our experimental diffraction data allow a calculation of the three partial atom-atom correlations of liquid HI. The main results are the following.

(1) There is no detectable evidence of H bonding in such a liquid.

(2) The anisotropic terms in the HI intermolecular potential do not appear to influence the center-center pair correlations. This evidence together with molecular-dynamics results for liquids composed of homonuclear diatomic molecules [14] suggests that anisotropic overlap contributions in the intermolecular potential should indeed be negligible in HI and that the only noticeable anisotropic contributions are therefore those due to electric multipoles.

(3) These anisotropic contributions influence the structure of the fluid only through the onset of a noticeable amount of correlation between the orientation of the molecular axes of different molecules. These correlations

TABLE V. Intermolecular partial pair distribution function of liquid HI.

r	$g_{\mathrm{HH}}(r)$	$g_{\mathrm{HI}}(r)$	$g_{\mathrm{II}}(r)$	r	$g_{\mathrm{HH}}(r)$	$g_{\mathrm{HI}}(r)$	$g_{\mathrm{II}}(r)$
0.00	0.000	0.000	0.000	4.88	0.966	1.136	1.784
0.40	0.000	0.000	0.000	5.03	0.974	1.138	1.536
0.80	0.000	0.000	0.000	5.13	0.986	1.137	1.352
1.20	0.000	0.000	0.000	5.24	1.001	1.132	1.143
1.60	0.000	0.000	0.000	5.34	1.016	1.125	1.000
2.01	0.003	0.050	0.000	5.45	1.025	1.114	0.907
2.11	0.010	0.262	0.000	5.56	1.029	1.100	0.863
2.20	0.009	0.337	0.000	5.67	1.031	1.080	0.835
2.31	0.095	0.385	0.000	5.79	1.031	1.052	0.814
2.41	0.244	0.378	0.000	5.90	1.030	1.014	0.786
2.51	0.388	0.380	0.000	6.02	1.032	0.972	0.739
2.61	0.523	0.418	0.000	6.14	1.034	0.939	0.680
2.71	0.649	0.474	0.000	6.27	1.035	0.918	0.631
2.80	0.767	0.528	0.000	6.39	1.035	0.906	0.602
2.91	0.921	0.597	0.000	6.52	1.034	0.901	0.593
3.00	1.012	0.641	0.000	6.65	1.030	0.901	0.601
3.12	1.077	0.695	0.000	6.78	1.024	0.904	0.630
3.21	1.089	0.742	0.000	6.92	1.015	0.912	0.689
3.31	1.089	0.799	0.000	7.06	1.006	0.924	0.780
3.41	1.093	0.868	0.000	7.20	1.000	0.937	0.867
3.52	1.105	0.946	0.000	7.35	0.996	0.951	0.936
3.62	1.122	1.008	0.000	7.50	0.994	0.965	0.997
3.70	1.129	1.037	0.000	7.65	0.992	0.984	1.070
3.81	1.134	1.064	0.349	7.80	0.989	1.006	1.144
3.92	1.121	1.083	0.755	7.96	0.987	1.025	1.194
4.00	1.103	1.095	1.128	8.12	0.987	1.036	1.213
4.12	1.061	1.109	1.751	8.28	0.987	1.043	1.217
4.29	1.003	1.114	2.302	8.45	0.988	1.047	1.211
4.42	0.979	1.118	2.342	8.62	0.990	1.047	1.194
4.51	0.973	1.119	2.295	8.79	0.995	1.045	1.162
4.60	0.971	1.119	2.215	9.33	1.006	1.023	0.998
4.69	0.970	1.124	2.096	9.71	1.007	0.996	0.913
4.79	0.967	1.130	1.946	10.10	1.004	0.977	0.895

appear in the partial structure factor $S_{\mathrm{HH}}(Q)$ and are those which determine the value of the Kirkwood correlation factor.

We want to point out that these conclusions have been reached by the determination of three partial structure factors and they could have hardly been achieved by an analysis of a single diffraction measurement.

More detailed information on the local molecular configurations responsible for the orientational correlations observed in these systems can be achieved by a proper modeling of $g(r_{12},\omega_1,\omega_2)$ and by computer simulation experiments [15]. Work is in progress in this direction keeping in mind that, using computer experiments for such purposes, one must always be sure that the adopted potential model is able to reproduce the experimental partial structure factors.

[1] L. Pauling, in *The Nature of the Chemical Bond and the Structures of Molecules and Crystals,* 2nd ed., edited by H. Milford (Cornell University Press, Ithaca, NY, 1945).

[2] M. Deraman, J. C. Doe, J. G. Powles, J. H. Holloway, and P. Chieux, Mol. Phys. **55**, 1351 (1985).

[3] A. K. Soper and P. A. Egelstaff, Mol. Phys. **42**, 399 (1981).

[4] J. G. Powles, E. K. Osae, J. C. Dore, and P. Chieux, Mol. Phys. **43**, 1051 (1981).

[5] J. G. Powles, E. K. Osae, J. C. Dore, J. H. Clarke, P. Chieux, and S. Cummings, Mol. Phys. **44**, 1131 (1981).

[6] C. G. Gray and K. E. Gubbins, *Theory of Molecular Fluids* (Clarendon, Oxford, 1984), Vol. 1, Chap. 3.

[7] *Comprehensive Inorganic Chemistry,* edited by A. F. Trotman-Dickenson (Pergamon, New York, 1973), Vol. 2, p. 1294.

[8] A. K. Soper, in *Proceedings of the Conference on Advanced Neutron Sources 1988,* edited by D. K. Hyer, IOP Conf. Proc. No. 97 (Institute of Physics and Physical Society, London, 1989), p. 353.

[9] A. K. Soper, W. S. Howells, and A. C. Hannon, Rutherford Appleton Laboratory Report No. 89-046, 1989 (unpublished); A. K. Soper and A. Luzar (unpublished).

[10] MINUIT version 9.7 of D1516-CERN Computer 7600 interium program library (1972).

[11] *Comprehensive Inorganic Chemistry* (Ref. [7]), p. 1290.

[12] L. Y. Wong and A. Anderson, J. Opt. Soc. Am. **62**, 1112 (1972).

[13] S. Murad, K. E. Gubbins, and J. C. Powles, Mol. Phys. **40**, 253 (1980).

[14] C. G. Gray and K. E. Gubbins, *Theory of Molecular Fluids* (Ref. [6]), Vol. I, Chap. 4, p. 272, Fig. 4.12.

[15] A. De Santis, A. Gregori, and D. Rocca, Chem. Phys. Lett. **181**, 579 (1991).